STEM CELLS AND DEVELOPMENT
Volume 29, Number 1, 2020

DOI: 10.1089/scd.2019.0169

Stem Cells from Human Trabecular Meshwork Hold the Potential to Develop into Ocular and Non-Ocular Lineages After Long-Term Storage

Ajay Kumar,[1] Yi Xu,[1] and Yiqin Du[1–3]

Stem cells from the eye hold a great potential for vision restoration and can also be used for regeneration in other tissues. In this study, we characterized the stem cell properties of Trabecular meshwork stem cells (TMSCs) after long-term cryopreservation (~8 years). TMSCs derived from four donors were examined for their viability and proliferation, as well as stem cell marker expression. Spheroid formation, colony formation, and multipotency were investigated. We observed that TMSCs were fully viable with variable proliferation ability. They expressed the stem cell markers CD90, CD166, CD105, CD73, OCT4, SSEA4, Notch1, *KLF4*, *ABCG2*, Nestin, and HNK1 detected by flow cytometry, quantitative polymerase chain reaction, or immunofluorescent staining. They could form spheroids and colonies after thawing. All TMSCs were able to differentiate into osteocytes, neural cells, and trabecular meshwork (TM) cells, but not adipocytes. Differentiated TM cells responded to dexamethasone treatment with increased expression of *myocilin* and angiopoietin-like 7 (*ANGPTL7*). In a nutshell, our study demonstrated that TMSCs retain their stem cell properties after long-term cryopreservation and hence can be an effective cell therapy source for various clinical applications.

Keywords: stem cells, cryopreservation, regeneration, multipotency, trabecular meshwork

Introduction

Glaucoma is among the leading causes of irreversible blindness, which is largely attributed to its asymptomatic nature at an early stage [1]. The main cause of glaucoma is increased outflow resistance, which could lead to elevated intraocular pressure (IOP) [2,3]. Reduction in cellularity of the trabecular meshwork (TM) contributes to the development of outflow resistance [4–6]. According to the National Institute of Health audacious goals initiative, stem cell therapy has been proposed to be an important tool for reversing vision loss due to glaucoma [7]. For clinical implication, adult tissue-specific stem cells offer a good source due to their feasibility for autologous transplantation [8,9].

Our group reported the successful isolation and characterization of trabecular meshwork stem cells (TMSCs) and demonstrated that these cells can successfully differentiate into TM cells in vitro [10,11]. TMSCs displayed the ability to home to the TM tissue and differentiate to TM cells in vivo [12]. These TMSCs were able to specifically home to laser-damaged TM tissue and regenerate the damaged tissue in vivo [13]. Progenitor cells from the TM have been suggested as an impending source for the advancement of personalized stem cell therapy for glaucoma [14]. After recruitment of the patients for different stem cell-based clinical trials, physicians need to administer repeated doses of stem cells at different time intervals [15].

To prevent the introduction of substantial manipulation due to laboratory culture conditions, stem cells are generally cryopreserved for later use. A very interesting study by Food and Drug Administration (FDA) reported that over 80% of the mesenchymal stem cell (MSC)-based product regulatory submissions included cryopreservation for storage and transportation before patient applications [16]. Functionality of MSCs post-thaw have been described as the main challenge by stem cell researchers [17], hence assessing the viability of MSCs is a commonly employed test post-thaw. However, viability is not a direct indicator of functionality and other tests should also be performed to assess functionality.

Cryopreservation stress may affect the stem cell viability and functionality, which can compromise the immunosuppressive properties of stem cells and may lead to failure of clinical trials [18]. Different facilities all around the world use different protocols for cryopreservation and this may be a determining factor for success or failure of a stem cell therapy. The most famous case includes failure of an MSC product named prochymal, which was implicated in Graft-versus-Host-Disease, while a similar trial became successful in Europe. One of the reasons for the failure was suggested

Departments of [1]Ophthalmology and [2]Developmental Biology, University of Pittsburgh, Pittsburgh, Pennsylvania.
[3]McGowan Institute for Regenerative Medicine, University of Pittsburgh, Pittsburgh, Pennsylvania.

to be stem cell damage due to cryopreservation, in addition to the donor heterogeneity, culture expansion, and immunogenicity [17].

Since TMSCs hold great promise as a suitable candidate for future stem cell therapy, characterization of their stemness and regenerative potential after long-term cryopreservation holds a great importance and can provide a suitable reference for use of these cells in designing of any future cell-based therapies in clinical trials.

Methods

Cell cryopreservation and revival

Cells were obtained from four deidentified corneas from the Center for Organ Recovery and Education (CORE, Pittsburgh, PA) with limited donor information mentioned in Supplementary Table S1. Written informed consent for use of cornea in research was obtained from all the donors by the CORE. All methods were performed in accordance with the relevant guidelines and regulations as laid by University of Pittsburgh and under an IRB-exempt protocol approved by University of Pittsburgh. Cells were cultured as reported previously [10] in Opti-MEM (Invitrogen, Carlsbad, CA) with different supplements, including epidermal growth factor (EGF, 10 ng/mL; Sigma-Aldrich, St. Louis, MO), bovine pituitary extract (100 μg/mL; Life Technologies, Carlsbad, CA), fetal bovine serum (FBS; 5%; ThermoFisher, Pittsburgh, PA), chondroitin sulfate (0.08%), ascorbic acid (20 μg/mL), and calcium chloride (200 μg/mL; Sigma-Aldrich) with antibiotics penicillin (100 IU/mL), streptomycin (100 μg/mL), and gentamicin (50 μg/mL; ThermoFisher). The medium was replenished every third day. Cells were passaged at 70%–80% confluence. Approximately 1×10^6 TMSCs per vial in 70% Dulbecco's modified Eagle's medium (DMEM)/F12, 20% FBS and 10% dimethyl sulfoxide (DMSO; ThermoFisher) were cryopreserved in a Mr. Frosty Freezing container at −80°C, allowing graduate temperature reduction overnight and then in liquid nitrogen for the duration of about 8 years. Cells were thawed by incubating in a prewarmed water bath at 37°C for fast temperature increase and removed DMSO by centrifugation, followed by suspension in T75 (75 cm^2) culture flasks in the above-mentioned culture medium.

Trypan blue exclusion assay

Immediately after thawing, TMSC suspensions were stained with trypan blue (Life Technologies) and viability was measured at least in triplicates. Cells were diluted in culture media, centrifuged (1,000 rpm, 5 min), and suspended in the complete culture medium by careful pipetting to avoid any mechanical damage. Countess II FL (Life Technologies) automated cell counter was employed to measure the percentage of viable and dead cells in the cell suspension. The percentage was calculated automatically based on exclusion or uptake of trypan blue (dead).

MTT assay

For the evaluation of cell viability by MTT assay, 5×10^3 cells were seeded into a 96-well plate and incubated for 48 h. Four hours before endpoint, MTT reagent (Millipore, Burlington, MA) was added in the wells at a 10% concentration and subsequent incubation was done in dark. After 4 h, cells were lysed with 100 μL of DMSO to release formed formazan crystals. The absorbance of the resulting solution was read at 570 nm measurement wavelength using 600 nm as a reference wavelength. Final optical density represents measurement wavelength minus reference wavelength. Cell viability was derived from these values using TMSC1 as the control.

Alamar blue assay

Equal number of TMSCs was seeded into culture plates and grown in Opti-MEM with supplements as mentioned above. After 48 h, cells were incubated with 10% Alamar blue (Bio-Rad, Hercules, CA). Alamar blue was converted subsequently into a red color compound due to the reaction in healthy metabolically active cells. Absorbance values were recorded at 570 nm measurement wavelength with 600 nm as a reference wavelength.

Annexin V/7-AAD staining

TMSCS were grown up to 70%–80% confluence and trypsinized as single cell suspension and washed with phosphate buffered saline (PBS). The cell pellet was obtained by centrifugation at 1,500 rpm for 5 min and cells were resuspended in Annexin V binding buffer. For evaluation of cell death, TMSCs were incubated with Annexin V and 7-AAD (BD Biosciences, San Jose, CA) simultaneously and incubated in dark for 15 min, and acquired in FACS Aria instrument immediately. At least 2×10^4 events were acquired per sample. Proper controls were unstained, Annexin V alone, and 7-AAD alone treated cells. Cells were suspended gently to avoid any cell death due to mechanical injury.

Calcein/Hoechst staining

Cells were cultured in T75 flasks at a density of 3×10^5 cells per flask and stained together with the viability stains Calcein (1:1,000) and Hoechst 33342 (1:2,000; Invitrogen) for 15 min. Cells were photographed employing excitation wavelength of 565 and 361 nm, respectively, using microscope model TE 200-E from Nikon Eclipse.

Flow cytometry

Cells were washed with PBS after detachment with TrypLE™ Express Enzyme (ThermoFisher). Nonspecific antibody sites were blocked by treating cells with 1% bovine serum albumin (BSA). The single cell suspension was treated with antibodies conjugated with different fluorochromes: FITC (Fluorescein Isothiocyanate), PE (Phycoerythrin), APC (Allophycocyanin), AF (Alexa Fluor)-488 or 647, and BV (Brilliant Violet) and incubated for a 30-min duration on ice in dark. Specific antibodies used are as following: CD90-BV510, CD166-FITC, CD105-AF647, CD73-PECY7, OCT4-FITC, SSEA4-AF488, Notch1-PE, CD34-FITC, and CD45-PE. Approximately 5×10^4 events were acquired per run on BD FACS Aria (BD Biosciences). Proper unstained controls and isotype controls were used for the experiments. The analysis was performed using the FlowJo_V10 software (FlowJo, Ashland, OR). The details about antibodies used in flow cytometry have been provided in Supplementary Table S2.

Quantitative polymerase chain reaction analysis

Cells were lysed in RLT buffer and RNA isolation was done using RNeasy kit from Qiagen (Hilden, Germany), as per manufacturer's instructions. DNase I treatment was given to avoid any DNA contamination. Complementary DNA (cDNA) was reverse transcribed from RNA. SYBR green chemistry was employed to assess the expression of different genes by quantitative polymerase chain reaction (qPCR). 18S ribosomal RNA (rRNA) was used as the housekeeping control. Ct values of genes of interest were subtracted from Ct values of 18S rRNA and were expressed as $2^{-\Delta Ct}$ as previously described [19]. Primers were designed on Primer3 website and the sequences are as follows: *18S* (forward: CCCTGTAATTGG AATGAGTCCAC; reverse: GCTGGAATTACCGCGGCT), *OCT4* (forward: GTGGAGGAAGCTGACAACAA; reverse: GGTTCTCGATACTGGTTCGC), *ABCG2* (forward: GCAG GGACGAACAATCATCT; reverse: CCTGAGGCCAATAA GGTGAG), *KLF4* (forward: ACCCTGGGTCTTGAGGA AGT; reverse: TGCCTTGAGATGGGAACTCT), *CHI3L1* (forward: CCTTGACCGCTTCCTCTGTA; reverse: GTGT TGAGCATGCCGTAGAG), *AQP1* (forward: CTGCACAGG CTTGCTGTATG; reverse: TGTCCTTGGGCTGCAACTA), *MYOC* (forward: AAGCCCACCTACCCCTACAC; reverse: TCCAGTGGCCTAGGCAGTAT), and *ANGPTL7* (forward: GCACCAAGGACAAGGACAAT; reverse: GATGCCATC CAGGTGCTTAT).

Colony-forming efficiency

To assess the colony-forming efficiency of cryopreserved TMSCs, thawed cells were allowed to attach and proliferate until 70%–80% confluence and then trypsinized with TrypLE. After dissociation and neutralization with medium containing FBS, cells were seeded at a density of 1×10^3 cells per well of six-well plates and allowed to proliferate in complete culture medium for 7 days. Colonies were fixed and stained with 0.1% crystal violet stain (Sigma-Aldrich). Stained colonies were counted manually under the light microscope. After counting, the stain was extracted using methanol and absorbance measured at 570 nm using a microplate reader (Synergy 2; BioTek, Winooski, VT).

Spheroid formation assay

Ultra-low attachment plates were utilized for this assay. Around 1×10^3 cells as single cell suspension were seeded per well of a 24-well plate. Cells proliferated and formed spheroids in days. Temporal photography of spheroids was done using EVOS XL core microscope (Life Technologies) and the area was measured using ImageJ software. At least 10 spheres in each condition were measured and averaged. For the medium change, spheroids were centrifuged at 1,000 rpm for 5 min and the pellet was suspended in fresh media. Spheroids were characterized for viability on day 66 by Calcein/Hoechst staining.

Multilineage differentiation

For osteogenic and adipogenic differentiation, 1×10^4 cells were seeded in 12 well plates. Cells were subjected to be induced for differentiation after achieving 70% confluence. Cells were induced in osteogenic or adipogenic differentiation media (Invitrogen). Cells were cultured in the complete differentiation media for 21 days. Osteogenic differentiation was confirmed by staining the mineralized granules with Alizarin red (Sigma-Aldrich), which was later extracted by cetylpyridinium chloride (CPC) buffer (Sigma-Aldrich) and quantified by measuring absorbance at 570 nm. Oil Red O stain was used to characterize the adipogenic differentiation of various TMSCs. Neural differentiation was achieved by culturing cells for 5 weeks in a differentiation medium composed of neurobasal media plus B27 supplement, epidermal/fibroblast growth factors (20 ng/mL), and N2 supplement (100×; Invitrogen) as reported previously [20,21]. Post differentiation, cells were stained using anti-Neurofilament and anti-β-III Tubulin antibodies (details in Supplementary Table S2). For TM cell differentiation, TMSCs were shifted from Opti-MEM to DMEM: HAM's F12 (1:1) medium with 10% FBS. Cells were induced for 10 days. TM differentiation was characterized by immunofluorescent staining and qPCR for CHI3L1 and AQP1. To test the response to dexamethasone (Dex; Sigma-Aldrich), these differentiated cells were treated with 100 nM of Dex for 10 days and were analyzed for myocilin expression by immunofluorescent staining and *myocilin* and *ANGPTL7* gene expression by qPCR.

Immunofluorescent staining

Cells were fixed with 4% paraformaldehyde and permeabilized by treating with 0.2% Triton X (ThermoFisher) for 15 min. Nonspecific sites were blocked using 1% BSA for 1 h. Neurofilament, β-III tubulin, CHI3L1, AQP1, and myocilin were used at 1:100 dilutions and incubated overnight at 4°C. Corresponding secondary antibodies were used at dilutions of 1:1,500 and incubated at room temperature for 2 h. DAPI (Sigma-Aldrich) was employed as a nuclear stain. Imaging was done using a confocal microscope (IX81; Olympus, Center Valley, PA). The same settings were used for each individual antibody staining and the mean fluorescence intensity (MFI) was calculated using ImageJ (provided in public domain, NIH, Bethesda, MD). A detailed list of all the antibodies used in the study is provided as Supplementary Table S2. For in vivo demonstration of TM regeneration, old slides maintained at −20°C from a laser damaged mouse model with transplanted TMSCs from a previous study [13] were used. At least six sections were stained for CHI3L1 and AQP1.

Statistical analysis

All statistical comparisons were made with primary TM cells or with TMSC1 as the reference. Results are represented as mean ± standard deviation. Data were statistically analyzed using one-way analysis of variance followed by Tukey posttest on SAS statistical package. P value <0.05 was considered statistically significant.

Results

Viability and proliferation of TMSCs after long-term cryopreservation

As evidenced by trypan blue exclusion assay, all TMSC strains showed >75% cell viability immediately post-thaw (Supplementary Fig. S1a). TMSC1 and TMSC3 displayed

higher cell viability (>95%) compared to TMSC2 and TMSC4. However, the TMSCs showed no significant difference in their cell viability based on Calcein/Hoechst staining, MTT assay, and Annexin V/7-AAD staining after cultivation. As shown in Supplementary Fig. S1b, TMSCs took both viability stains, Calcein and Hoechst. MTT assay showed no significant difference of cell viability between all four TMSCs (Supplementary Fig. S1c). Cell death detection by Annexin V/7-AAD staining showed that TMSC1 and TMSC4 underwent little apoptosis as indicated by Annexin V uptake; however, TMSC2 (4.76 ± 1.5) and TMSC3 (9.3 ± 0.84) showed increased apoptosis (Supplementary Fig. S2a, b). 7-AAD, which penetrates nonviable cells binding to DNA and is excluded from live cells with intact cell membranes, showed a significantly increased uptake in TMSC2 (3.58 ± 0.46), TMSC3 (3.1 ± 0.11), and TMSC4 (3.44 ± 0.45) compared to TMSC1 (0.44 ± 0.94). TMSC2 showed a significantly higher proliferation rate compared to other three TMSCs, while TMSC4 showed the least proliferation rate (Supplementary Fig. S2c) as indicated by Alamar blue cell proliferation assay. To summarize, TMSCs maintained a significant viability and comparable proliferation after long-term cryopreservation.

Expression of stem cell markers in cryopreserved TMSCs

We characterized the cryopreserved TMSCs for their stemness depending on the stem cell marker expression profile by flow cytometry and immunofluorescent staining, or by qPCR. Flow cytometry results showed a significant difference among different TMSCs. As shown in Fig. 1a and b, TMSC1 showed a significantly higher expression of CD90 (95.8%), CD73 ($89.8\% \pm 1\%$), CD105 ($73.3\% \pm 1\%$), OCT4 ($79.4\% \pm 2.7\%$), and SSEA4 ($80.2\% \pm 0.5\%$) compared to other three TMSCs and primary cultured TM cells as negative control. TMSC4 showed the least expression of CD90 ($73.3\% \pm 0.72\%$), CD73 ($61.5\% \pm 1.9\%$), and SSEA4 ($42.3\% \pm 1.1\%$). TMSC3 had the least expression of CD105 ($45.6\% \pm 1.8\%$), OCT4 ($36.1\% \pm 2.6\%$), and CD166 ($44.8\% \pm 3.2\%$). Notch1 was expressed to a significantly higher level in TMSC2 ($11.8\% \pm 0.9\%$) compared to other three TMSCs, while CD34 and CD45 showed negligible expression. As a

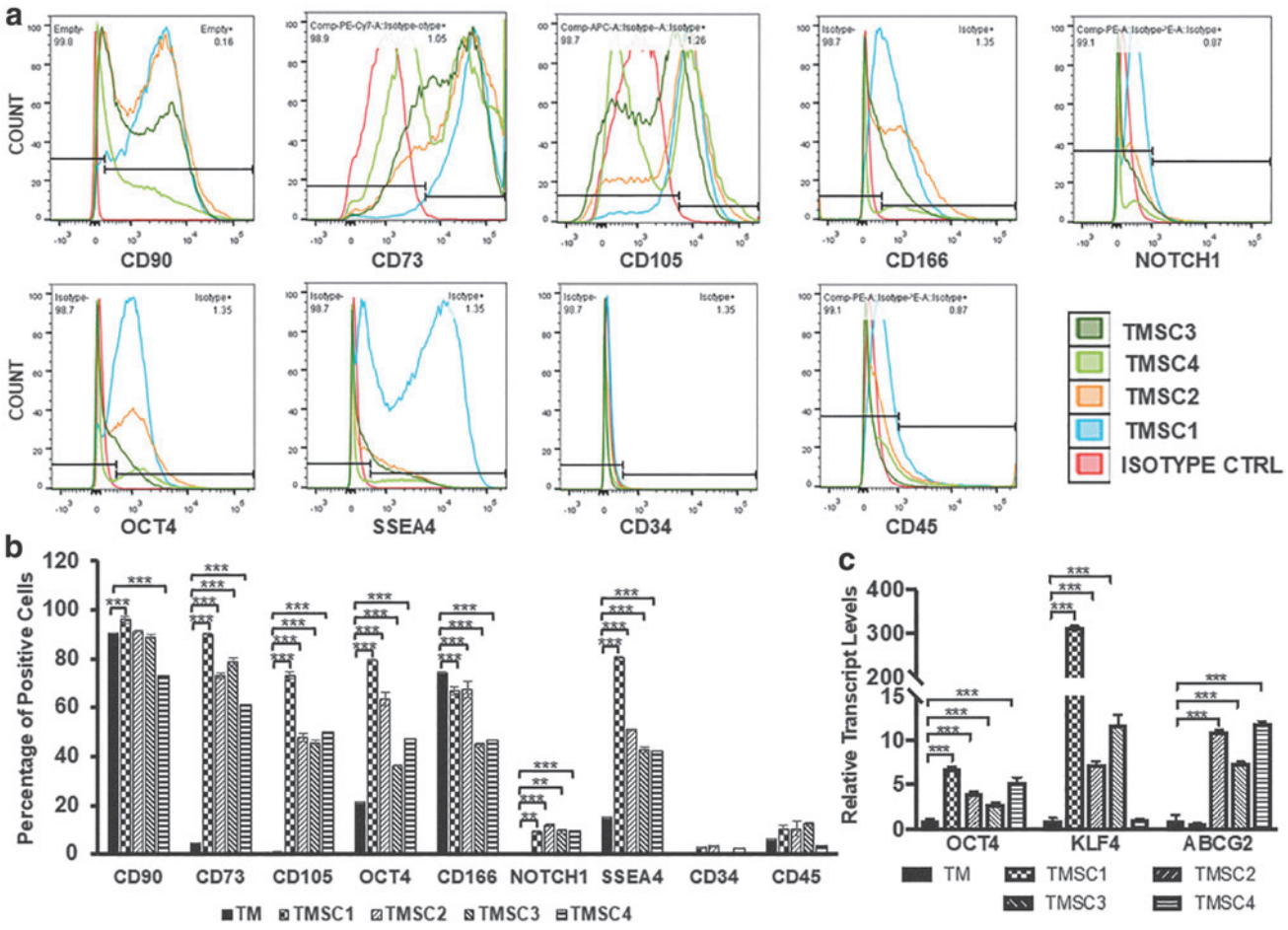

FIG. 1. Expression of stem cell markers in cryo-TMSCs after revival. **(a)** Flow cytometry histograms showing the positive percentage for different antibodies. **(b)** Bar diagram showing a comparison of stem cell marker expression of different TMSCs by flow cytometry, statistical comparison was made with reference to primary TM cells. **(c)** Bar diagram showing the qPCR results for various stem cell genes. Statistical comparison was made with reference to primary TM cells. $^{**}P < 0.001$, $^{***}P < 0.0001$. qPCR, quantitative polymerase chain reaction; TM, trabecular meshwork; TMSCs, trabecular meshwork stem cells. Color images are available online.

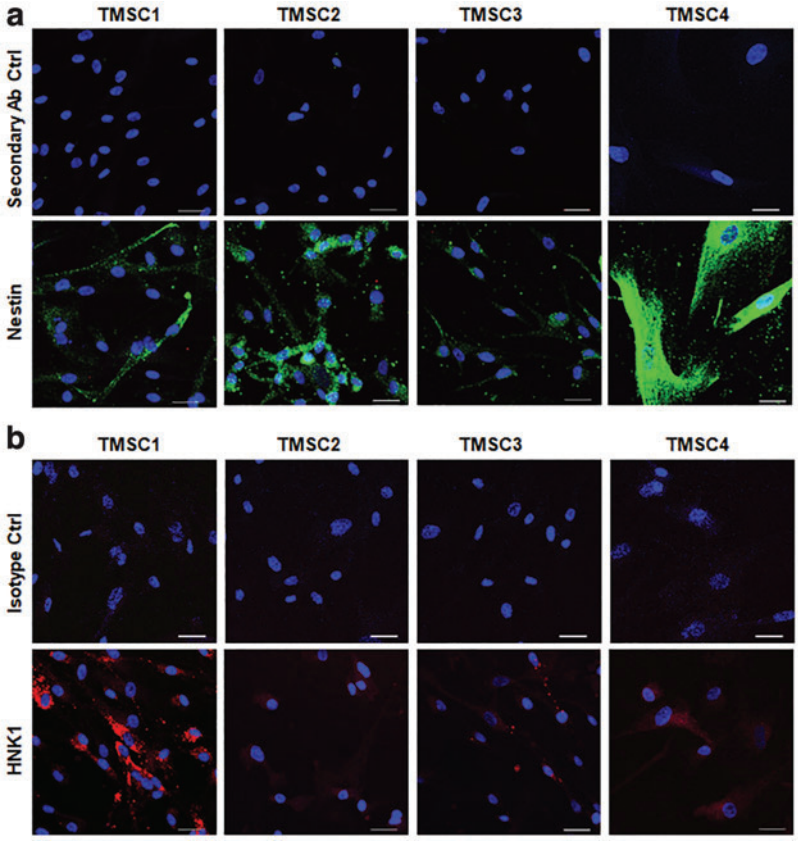

FIG. 2. Marker staining of cryo-TMSCs. **(a)** Confocal microscopy images showing the staining pattern for Nestin and secondary antibody controls in different TMSCs. **(b)** Staining for HNK1 and isotype controls. Scale bars, 30 μm. Color images are available online.

control, TM cells had various expression of these markers (CD90, 90.7% ± 0.1%; CD73, 4.8%; CD105, 1.2% ± 0.1%; OCT4, 21.6% ± 0.3%; CD166, 74.7 ± 0.3; Notch1, 0.2%; SSEA4, 15 ± 0.2; CD34 0.5% ± 0.1%; and CD45, 5.9% ± 0.5%). qPCR analysis showed that all the TMSCs expressed *OCT4*, *KLF4*, and *ABCG2* significantly higher compared to the primary TM cells (Fig. 1c). TMSC1 showed the highest expression of *OCT4* (6.8 ± 0.1) and *KLF4* (314.2 ± 2.5) while TMSC4 had the highest expression of *ABCG2* (11.9 ± 0.2) compared to the TM cells and other TMSCs. Immunofluorescent staining results indicated that these TMSCs were positive to Nestin and HNK1 (Fig. 2a, b). In summary, cryopreserved TMSCs maintained their stem cell markers on both protein and gene levels with some variations.

Colony-forming efficiency and spheroid formation potential of TMSCs

These two assays were performed by culturing the cells in adherent and ultra-low attachment plates, respectively. Colony forming assay showed a significant higher tendency of TMSC1 to form colonies (30.5 ± 4.1) compared to TMSC2 (16.5 ± 2.1), TMSC3 (20.5 ± 2.3), and TMSC4 (2 ± 0.63) (Supplementary Fig. S3a, b). The colony counts were confirmed by extracting out crystal violet stain from colonies using 100% methanol. The colonies derived from TMSC1 showed maximum uptake of crystal violet (optical density 0.75 ± 0.09) compared to TMSC2 (0.45 ± 0.06), TMSC3 (0.32 ± 0.03), and TMSC4 (0.33 ± 0.02) (Supplementary Fig. S3c). The spheroid formation potential was detected by culturing the cells in ultra-low attachment plates. TMSC1 formed the biggest spheroids (531.8 ± 32.5 μm^2) as evidenced by area measurements of spheroids in comparison with TMSC2 (288.1 ± 59.6 μm^2), TMSC3 (262.6 ± 261 μm^2), and TMSC4 (267 ± 32.5 μm^2) (Fig. 3a, c). Spheroids formed from all TMSCs were viable for more than 2 months as shown by Calcein/Hoechst uptake at 66 days of sphere culture (Fig. 3b). In contrast, very few TM cells formed spheroids of tiny size and those spheroids grew very slow as shown in Fig. 3d on days 1 and 5. In conclusion, all TMSCs retained their spheroid forming potential and colony-forming capacity, but very less colonies were formed in TMSC2.

Multipotency of cryopreserved TMSCs

We assessed the multipotent differentiation potential of revived TMSCs by inducing the cells to osteocytes, adipocytes, and neural cells. All four TMSCs were able to differentiate into osteocytes after 21-day induction. The differentiated cells were able to bind to alizarin red, which indicated the formation of mineralized calcium granules compared to undifferentiated control cells (Fig. 4a). All TMSCs showed a significant increase in alizarin red uptake after osteogenic differentiation compared to their undifferentiated controls (Fig. 4b). Comparison between differentiated TMSCs demonstrated the highest tendency of TMSC1 toward osteogenic differentiation as indicated by significantly high alizarin red uptake (3.9 ± 0.07) compared to TMSC2 (0.3 ± 0.03), TMSC3 (0.5 ± 0.01), and TMSC4 (0.3 ± 0.07). After induction in adipogenic differentiation medium for 21 days, none of the TMSCs were detected with any lipid droplets by Oil red O staining

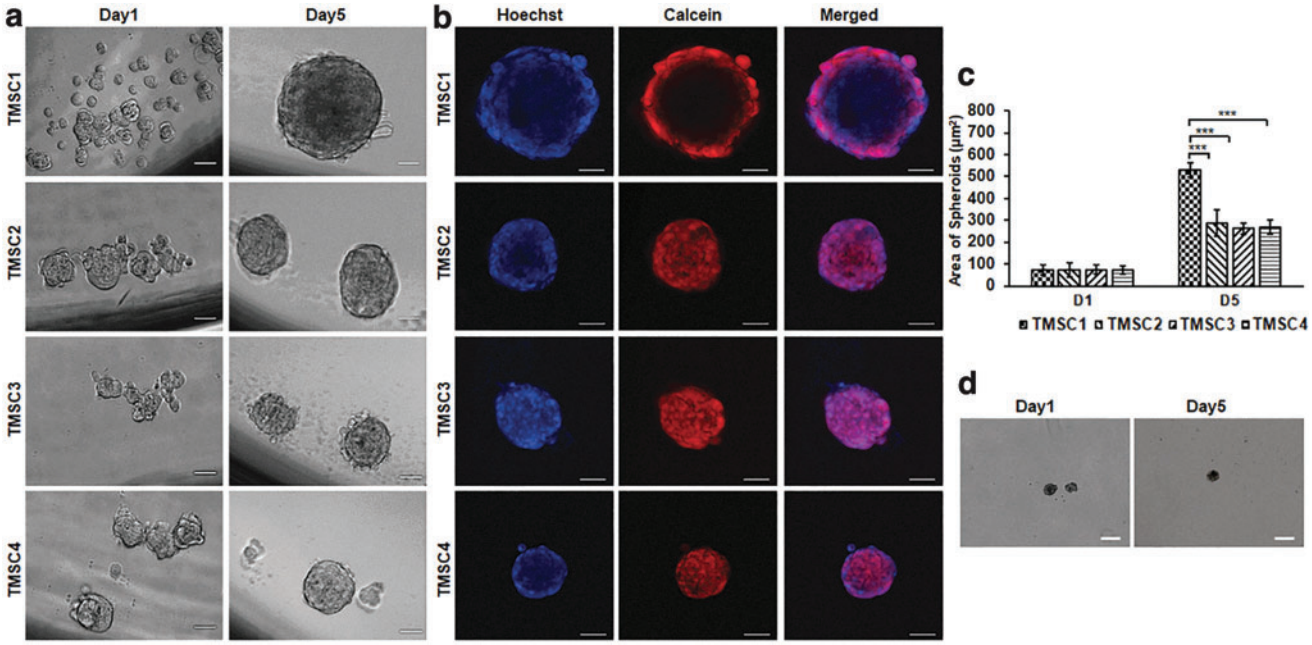

FIG. 3. Formation of spheroids. **(a)** Phase-contrast images of TMSC spheroids derived at days 1 and 5 of culture. **(b)** Calcein/Hoechst staining of spheroids derived from different TMSCs after 66 days of culture for viability testing. **(c)** Bar diagram showing comparative sphere size on days 1 and 5. **(d)** Phase-contrast images of spheroids formed by TM cells on days 1 and 5. Scale bars, 50 μm, Statistical comparison was made with reference to TMSC1. $^{***}P < 0.0001$. Color images are available online.

(Fig. 4c). This indicated that the cryopreserved TMSCs failed to be induced to adipocytes.

Evaluation of neural differentiation potential showed that all four TMSCs could differentiate into neural cells (Fig. 5). After 5-week induction, the differentiated TMSCs showed positive staining for neurofilament, while the undifferentiated control TMSCs were negative (Fig. 5a). MFI of neurofilament showed that all four TMSCs had increased expression of neurofilament after neural induction compared to undifferentiated cells (N-TMSC1, 60.5 ± 23.9; N-TMSC2,

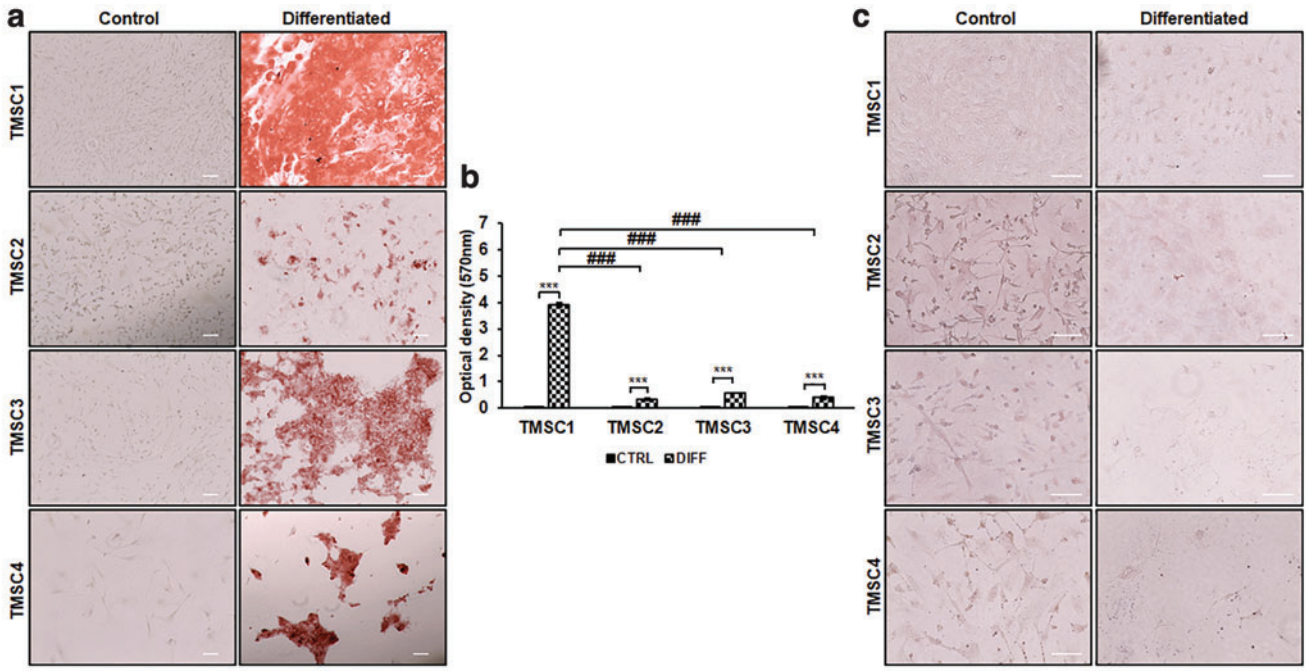

FIG. 4. Osteogenic and adipogenic differentiation potential of cryo-TMSCs. **(a)** Alizarin red stained undifferentiated (Control) and differentiated cells with osteogenic induction. **(b)** Bar diagram showing quantification of the optical density of stained alizarin red for osteogenic differentiation. ***Comparison between control and differentiated cells. ###Comparison between differentiated cell types with reference to TMSC1. $^{***/\#\#\#}P < 0.0001$. **(c)** Cells stained with Oil Red O post-adipogenic differentiation. Scale bars, 100 μm. Color images are available online.

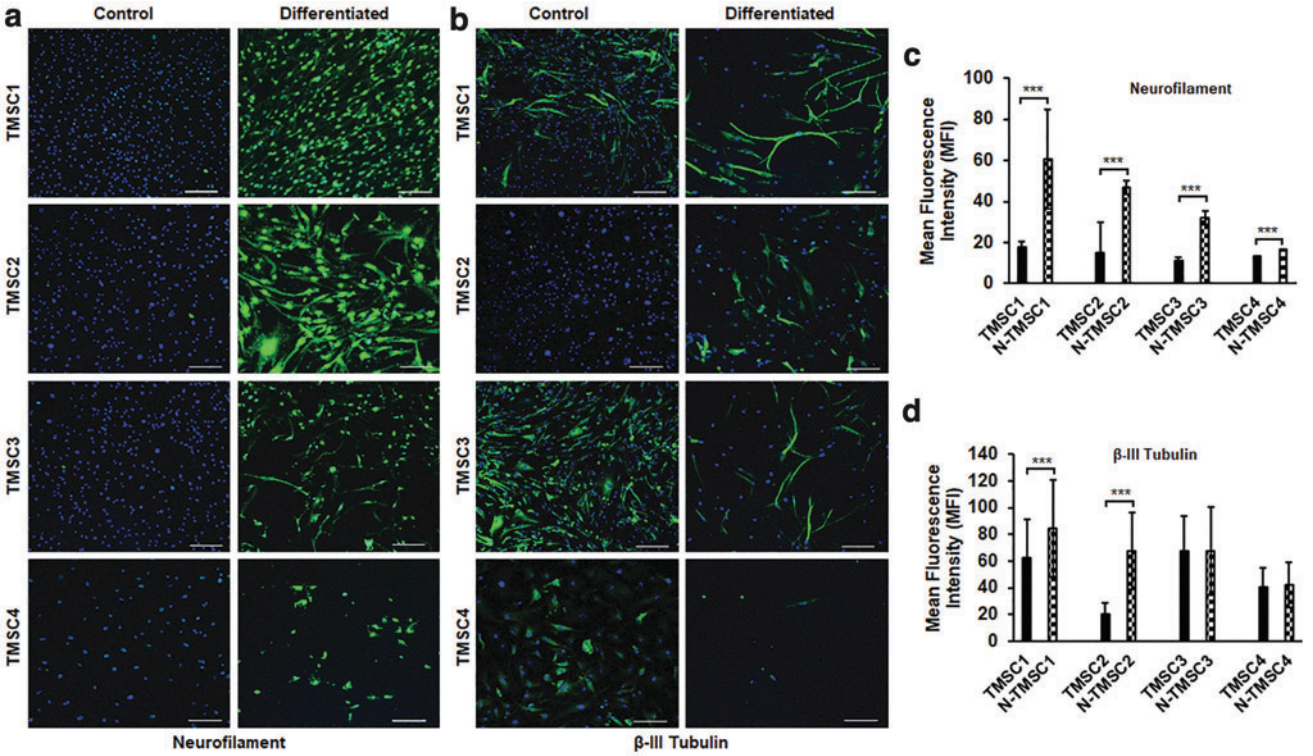

FIG. 5. Neural differentiation of cryo-TMSCs. **(a, b)** Confocal images showing immunofluorescent staining for neurofilament and β-III tubulin in control and neural differentiated cells. **(c, d)** Bar diagram showing difference in MFI for neurofilament and β-III tubulin between control and neural differentiated (N-TMSC1 and so on) TMSCs. The images were taken at the same settings. Scale bars, 200 μm. ***$P < 0.0001$. MFI, mean fluorescence intensity. Color images are available online.

46.7 ± 14.7; N-TMSC3, 32.2 ± 6.5; and N-TMSC4, 16.4 ± 3.2) (Fig. 5c). The TMSCs in both undifferentiated and differentiated states demonstrated positivity for β-III tubulin (Fig. 5b). However, the MFI was significantly higher in differentiated N-TMSC1 (84.5 ± 36.4) and N-TMSC2 (67.4.4 ± 28.8) compared to control TMSC1 (62.7 ± 28.2) and TMSC2 (20.1 ± 8.4), while no significant difference was observed for TMSC3 and TMSC4 (Fig. 5d). It may also be noted that the neural differentiation is evident from distinct neuronal morphology of the cells post differentiation compared to the undifferentiated cells (Fig. 5a, b). Hence, multilineage potential evaluation demonstrated that TMSCs could successfully differentiate to osteocytes and neurons, but failed to form adipocytes post-thaw.

TM cell differentiation of cryopreserved TMSCs

TMSCs differentiating into TM cells for TM regeneration are an ultimate goal for treating glaucoma. TMSCs were induced for TM differentiation in 10 days. Immunofluorescent staining showed positive expression of TM cell markers AQP1 and CHI3L1 in differentiated cells (Fig. 6a). A quantitative analysis of the MFI showed that AQP1 expression was significantly increased in all TMSCs post-differentiation, except TMSC4 (Fig. 6b). CHI3L1 expression was significantly increased in all TMSCs post differentiation (Fig. 6c). qPCR analysis indicated a different trend among TMSCs. TM genes *AQP1* (220 ± 12.1) and *CHI3L1* (35.8 ± 1.2) were expressed highest in differentiated TMSC3 (Fig. 6d, e). Differentiated TMSC2 had increased expression of both *AQP1* (5.4 ± 0.8%) and *CHI3L1* (12.1% ± 0.1%). *AQP1* (0.05 ± 0.01) was expressed least in differentiated TMSC4, while *CHI3L1* was expressed least in TMSC1 (0.9 ± 0.1) (Fig. 6d, e).

Dex is known to induce glaucomatous transformation in TM cells and increased myocilin expression in response to Dex treatment is the most reliable way to identify TM cells [22]. To confirm the differentiated cells are TM cells, they were treated with 100 nM Dex for 10 days. As shown in Fig. 7a, the differentiated TM cells lost expression of AQP1 and reduced expression of CHI3L1 by immunofluorescent staining. Gene expression analysis by qPCR showed a significant reduction in *AQP1* in differentiated TM cells derived from TMSC3 (166 ± 18.1) and TMSC1 (5.5 ± 0.3) compared to their non-Dex-treated counterparts (556.9 ± 12.4 and 24.7 ± 1.3, respectively) (Fig. 7b). The expression reduction was not significant in differentiated TMSC2. Differentiated TMSC4 showed a slight increase in *AQP1* after Dex treatment (12.4 ± 0.1) in comparison to non-Dex-treated cells (11.2 ± 0.1) (Fig. 7b).

qPCR analysis for *CHI3L1* showed a significant reduction in differentiated TMSC1 after Dex treatment (0.09 ± 0.004) compared to non-Dex-treated cells (1.36 ± 0.07). Dex-treated differentiated TMSC2 and TMSC3 did not show significant changes after Dex treatment. However, differentiated TMSC4 showed a significant increase in *CHI3L1* (6.4 ± 0.1) after Dex in comparison to non-Dex-treated cells (4.9 ± 0.08) (Fig. 7c).

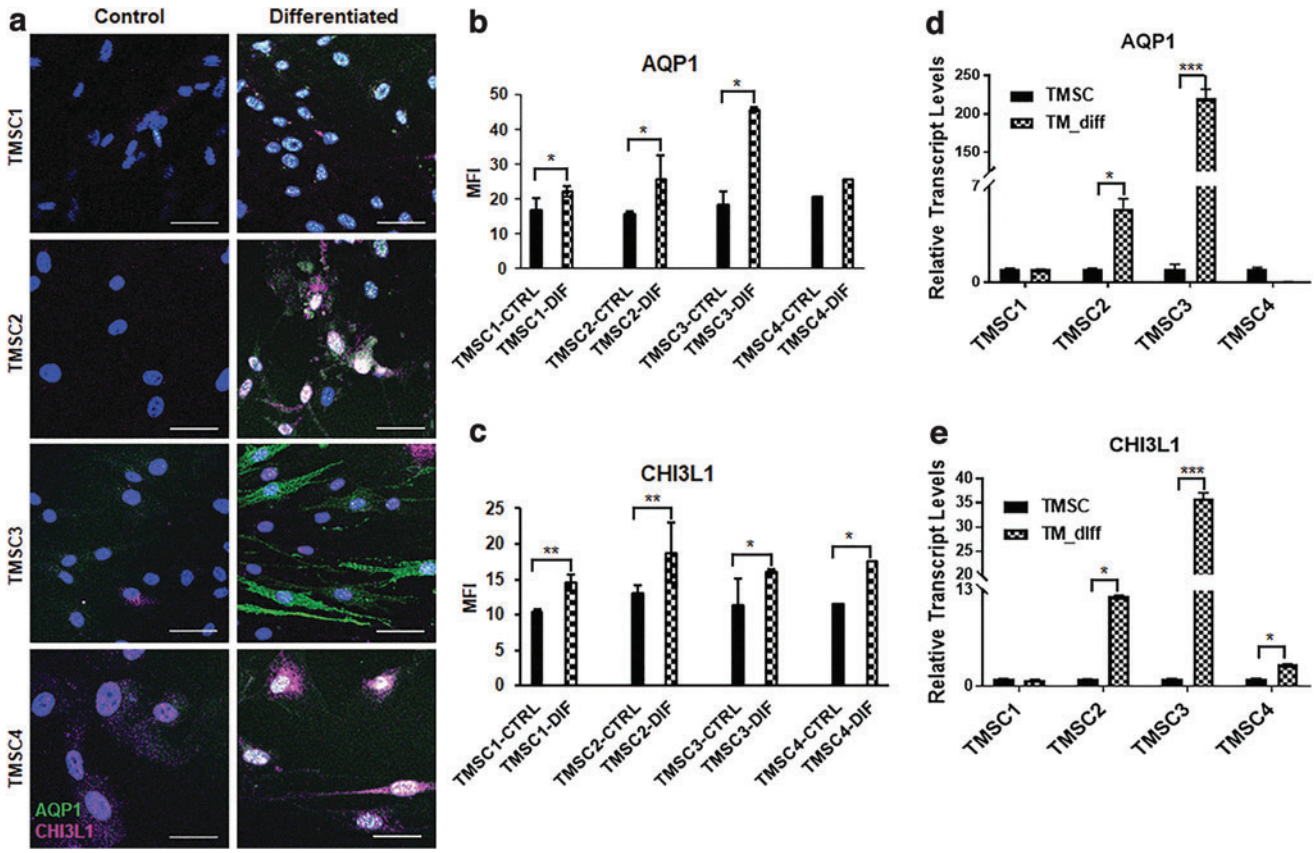

FIG. 6. TM cell differentiation of cryo-TMSCs. **(a)** Immunofluorescent staining of AQP1 (*green*) and CHI3L1 (*magenta*) in control and TM differentiated cells. Scale bars, 50 µm. **(b, c)** Quantification of MFI for AQP1 and CHI3L1, respectively, **(d, e)** qPCR analysis showing a comparison of the gene expression profile of TM markers AQP1 and CHI3L1 pre-/post-TM differentiation. $*P \leq 0.05$, $**P \leq 0.001$, $***P \leq 0.0001$. Color images are available online.

Immunofluorescent staining showed that the TM cells differentiated from TMSCs1, TMSC2, and TMSC3 increased their expression of myocilin after Dex treatment compared to non-Dex-treated cells and undifferentiated TMSCs (Fig. 8a). The differentiated TMSC4 with and without Dex treatment showed increased myocilin staining (Fig. 8a). qPCR analysis demonstrated a significantly increased expression in *myocilin* in all differentiated TM cells after Dex treatment as shown in Fig. 8b. *ANGPTL7* gene expression showed similar results to that of *myocilin* where *ANGPTL7* was increased to a

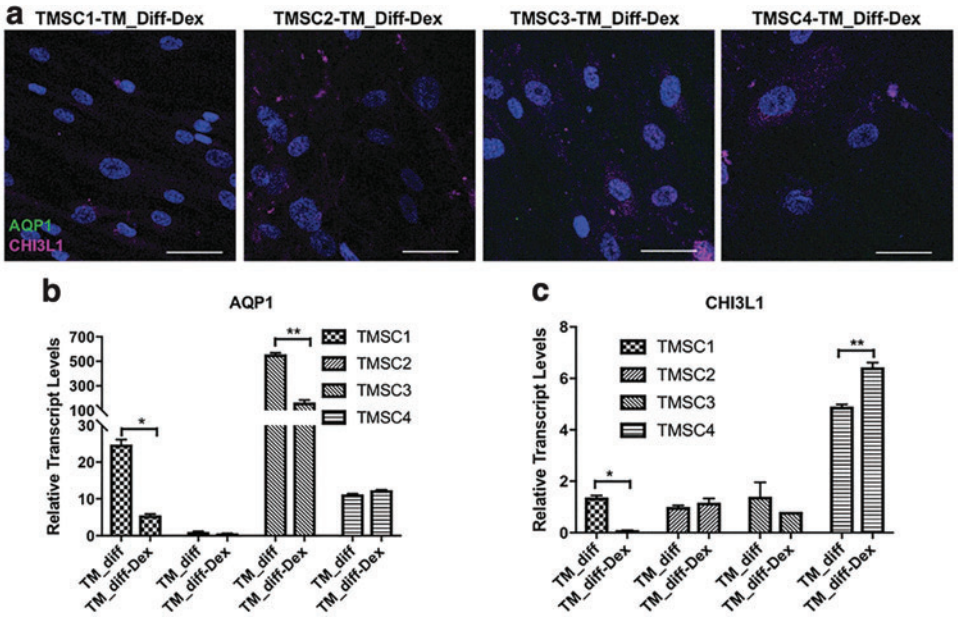

FIG. 7. Expression analysis of AQP1 and CHI3L1 in Dex-treated TMSCs after induction. **(a)** Immunofluorescent staining for AQP1 (*green*) and CHI3L1 (*magenta*) after Dex treatment for 10 days in differentiated TM cells from different TMSCs. **(b, c)** qPCR analysis for AQP1 and CHI3L1 in differentiated TM cells from different TMSCs with or without Dex treatment. Scale bars, 50 µm. $*P < 0.05$, $**P < 0.001$. Dex, dexamethasone. Color images are available online.

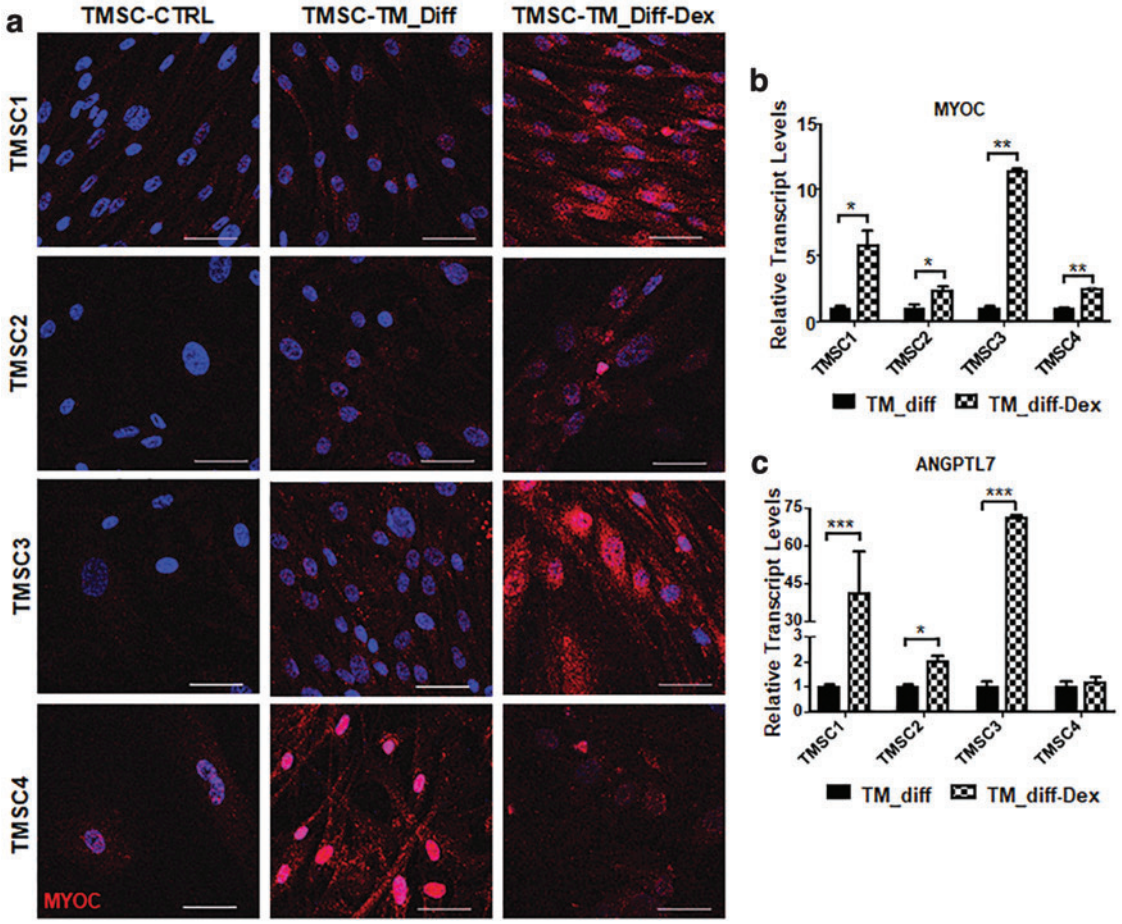

FIG. 8. Response to Dex treatment by TM cells derived from cryo-TMSCs. **(a)** Immunofluorescent staining for myocilin in control TMSCs, differentiated TMSCs (TMSC-TM_diff), and Dex-treated differentiated TMSCs (TMSC-TM_diff-Dex). **(b, c)** Bar diagram showing gene expression profile for myocilin and ANGPTL7 in differentiated cells from different TMSCs with or without Dex treatment. Scale bars, 50 μm. $*P < 0.05$, $**P < 0.001$, $***P < 0.0001$. ANGPTL7, angiopoietin-like 7. Color images are available online.

significant level in all Dex-treated differentiated TM cells, except TMSC4 (Fig. 8c), which showed no significant difference with and without Dex treatment.

Immunofluorescent staining on cryosections of laser-damaged mouse TM with long-term cryopreserved TMSC transplantation demonstrated that transplanted TMSCs could differentiate into TM cells in vivo as indicated by positive staining of AQP1 and CHI3L1, which are TM cell markers (Fig. 9).

To conclude, after long-term cryopreservation, all TMSCs could be easily induced to differentiate to TM cells, which indicate a potential for TM regeneration.

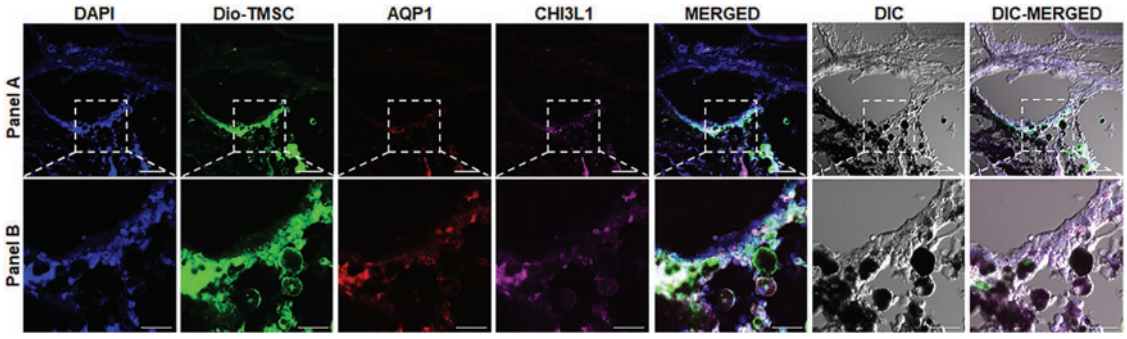

FIG. 9. TM regeneration by transplanted TMSCs. Transplanted TMSCs (Dio labeled shown as *green*) can differentiate into TM cells in vivo 2 weeks after transplantation into laser-injured mouse TM region, as indicated by co-staining of AQP1 (*red*) and CHI3L1 (*magenta*) with *green* TMSCs. DAPI stains nuclei blue. Scale bars, **(A)** 50 μm and **(B)** 20 μm. Color images are available online.

Discussion

In this study, we reported that long-term cryopreserved TMSCs averaging about 8 years from four different donors were maintaining cell viability, proliferation potential, expression of stem cell markers, multipotency, and the ability to differentiate into TM cells, which are responsive to Dex treatment. This study showed evidence that cryopreserved TMSCs could be a reliable source for stem cell-based therapy for TM regeneration and a reliable treatment option for glaucoma in the future.

Stem cell-based therapy as a tool for disease treatment is advancing day by day with occasional setbacks and fiascoes [23–25]. The effective dose of stem cells employed in different clinical trials ranges from a low dose of a million cells to a high dose of a billion cells [26–28]. These variations largely depend on the disease type, patient variability, and the physician's choice. Despite the dosing, stem cells are injected at different time points and require more than one administration. To cope with the high number of stem cells required to meet clinical demand and to prevent stem cell manipulation, it is important to cryopreserve stem cells. This can prevent any unwanted genetic aberrations and can also avoid repeated harvesting from patients. Deep understanding of stem cell biology and proper quality control under good manufacturing practices are essential before using these cells for any clinical transplantation.

Depending on the protocols applied in cryopreservation, cell type, and duration of storage, it is crucial to assess the quality of cells before using them for further downstream applications. This quality can be assessed by subjecting them to characterization based on genes, phenotype, and functional differentiation into various lineages. Since their discovery, TMSCs have been shown to display the multilineage differentiation potential [10] with the ability to home to and repair the damaged TM [12,13]. There are no data available regarding their regenerative potential post cryopreservation. Several studies have shown the loss of stem cell viability and functionality after cryopreservation [29,30], whereas others could not observe any significant cell death [31,32]. Although there was significant cell death in some of the studied TMSC strains postthaw in our study, after attachment, the cells showed no significant difference on cell viability and proliferation. The cryopreservation method we used is a very common protocol employed by many researchers all around the world and it does not have special advantages over existing cryopreservation protocols, although slow freezing and fast thawing are key factors for the process. Our study indicates the fidelity and rugged characteristics of TMSCs that they could successfully withstand long-term cryopreservation.

Colony formation is one of the assays for functional enumeration of the functionality of stem cells [33]. Higher colony-forming efficiency and proliferation of TMSC1 in comparison to other stem cell strains might be an indication of individual differences between different donors. Spheroid formation assay is used to characterize the self-renewal capacity of single stem cells in cellular system [20,34]. The corresponding tendency of TMSC1 cells to form bigger spheroids was consistent, similar to the colony formation and cell proliferation tendencies. Although TMSC1 were at passage 1 when frozen, earlier than the other TMSCs at passage 2 or 3, we still cannot conclude that earlier passaged cells were better than later passaged cells. Further study is needed to compare cells from same donors at different passages and with different frozen periods, so we can get a conclusion on the effects of passage number, age of donor, and times of cryopreservation on properties of TMSCs after long-term cryopreservation.

Stem cells/progenitors from the TM have been reported by several groups [10–13,35–41]. These stem cells/progenitors expressed embryonic stem cell markers OCT4, KLF4, Sox2, Nanog, Bmi1, MSC markers CD73, CD90, CD105, and CD166; neural stem cell markers Nestin and Pax6; and other stem cell markers ABCG2, Notch 1, Mucin 1, and Ankyrin G. These cells are multipotent with the ability to differentiate into different lineage cell types, such as osteocytes, adipocytes, chondrocytes, neural cells, keratocytes, and TM cells. In this study, we found that the cryopreserved TMSCs were positive to CD90, CD105, CD166, and CD73, as well as OCT4, Notch 1, SSEA4, KLF4, ABCG2, Nestin, and HNK1, but negative to CD34 and CD45. This demonstrates the maintenance of stem cell characteristics over prolonged storage and positive expression of Nestin and HNK1 may indicate their neural crest origin. However, TMSC4 displayed the consistent low expression of stem cell markers compared to other TMSCs, which may be related to individual differences between the donors.

Stem cells have been widely used for applications involving bone regeneration [42]. Since the discovery of TMSCs, several studies have shown the osteogenic potential of TMSCs [10,35,43]. Our study showed that cryo-TMSCs could maintain their osteogenic potential after long-term storage and can be used effectively for bone regeneration in preclinical and translational studies. In addition to osteocytes, TMSCs can also be differentiated into adipocytes robustly [10,11,40]. However, loss of adipogenic tendency of TMSCs after cryopreservation in all the four samples emphasizes the fact that TMSCs might not be a suitable cell type to be used in fat tissue reconstruction-based applications after cryopreservation.

Stem cell therapy has been demonstrated to show a therapeutic recovery in an array of neurodegenerative diseases [44] like amyotrophic lateral sclerosis [45], spinal muscular atrophy [46], and Huntington's [47]. Neurofilament is an essential cytoskeletal protein of mature neurons and its expression plays an important role in the nervous system development [48]. Neurofilament is important for neuronal growth and its decreased expression with age has been correlated with decreased neural regeneration in aged rats compared to young ones [49]. Tendency of cryo-TMSCs to differentiate into neuron-like cells post-cryopreservation offers a valuable tool for the use of stem cells in neurodegenerative diseases.

All TMSCs could successfully differentiate into neural cells post-thaw, which indicates their potential application for regeneration into neurodegenerative disorders. However, TMSC4 showed the least expression of neurofilament, which is correlated to the corresponding low stem cell marker expression and may arise due to individual differences between different donors. β-III tubulin is an early neuronal marker, but previous reports have demonstrated the positive expression of β-III tubulin in a number of progenitors obtained from skin, dental pulp, and periodontal

ligament [50]. This might explain the positivity of β-III tubulin observed in TMSCs at baseline, suggesting that β-III tubulin might express in some adult stem cells as a common marker and may not be just limited to neuronal cells. However, it may be noted that it expressed more potently post differentiation in some TMSCs and the neuronal morphology post differentiation was more conspicuous compared to undifferentiated cells.

TM cells play an important role in regulating the outflow facility and hence maintaining the proper IOP of the eye [11]. TM cellularity is highly reduced in glaucoma [4–6] and our group has shown that TMSCs can home to TM tissue in vivo [12] and contribute to the repair of damaged TM tissue [13]. CHI3L1 and AQP1 serve as important markers for TM cells [51,52]. AQP1 is reported to regulate resting intracellular volume and paracellular permeability of TM cell monolayers in vitro [53]. CHI3L1 plays a role in extracellular matrix remodeling in the TM tissue [10] and changes the expression levels in TMSCs in response to endoplasmic reticulum (ER) stress [54]. Increased expression of CHI3L1 and AQP1 in differentiated TMSCs indicated that all four TMSCs retained their ability to differentiate into TM cells after long-term storage. TMSC3 showed the highest increase of AQP1 and CHI3L1 after induction, which may be related to the young age of the donor. Further study is needed to confirm it.

Dex can induce glaucoma-like changes in cell culture conditions by increasing TM cell stiffness and elevating myocilin expression [55,56]. Responding to Dex with increased expression of myocilin is one of the characteristics of TM cells [22]. Angiopoietin-like 7 (ANGPTL7) has been reported to be elevated in aqueous humor in glaucoma patients, hence indicating its role in glaucoma pathogenesis [57,58]. Elevated expression of both *myocilin* and *ANGPTL7* in differentiated TM cells after Dex treatment emphasized an efficient differentiation of all four TMSCs to TM cells. The various changes of AQP1 and CHI3L1 in differentiated TMSCs after Dex treatment may indicate the variations of TM cell function in response to Dex treatment and cannot be an indicator of TM cell characteristics in response to Dex, while increased expression of myocilin is a reliable indicator of TM cell response to Dex.

We have previously shown that human TMSCs could integrate specifically to and repair laser-damaged TM tissue in mice [13]. The long-term cryopreserved TMSCs after transplantation expressing AQP1 and CHI3L1 confirmed that cryopreserved TMSCs can be successfully used to regenerate TM in vivo.

Conclusion

To conclude, TMSCs derived from four donors displayed and maintained their stem cell characteristics and function after long-term cryopreservation. Since TMSCs could be isolated and cultured from corneal rims discarded after corneal transplantation and be induced to differentiate into different cell types, TMSCs could offer a valuable source to be used for applications in regenerative medicine in the areas of bone-related disorders, neurodegenerative diseases, and ocular disorders. This study effectively demonstrates that TMSCs can withstand the long periods of cryopreservation and hence offers an impending source for stem cell therapy in the long run.

Acknowledgments

The authors acknowledge Ms. Kira Lathrop for confocal microscopy and Nancy Zurowski for flow cytometry.

Author Disclosure Statement

University of Pittsburgh has a competing interest with a patent named ''trabecular meshwork stem cells'' with Y.D. as one of the inventors. All other authors declare no competing financial interest.

Data Availability Statement

All article-related files and data are available with the corresponding author on reasonable request.

Funding Information

This work was supported by National Institutes of Health grants EY025643 (Y.D.), P30-EY008098, BrightFocus Foundation G2014086 (Y.D.), Research to Prevent Blindness; and Eye and Ear Foundation of Pittsburgh.

Supplementary Material

Supplementary Figure S1
Supplementary Figure S2
Supplementary Figure S3
Supplementary Table S1
Supplementary Table S2

References

1. Weinreb RN, T Aung and FA Medeiros. (2014). The pathophysiology and treatment of glaucoma: a review. JAMA 311:1901–1911.
2. Quigley HA, EM Addicks, WR Green and AE Maumenee. (1981). Optic nerve damage in human glaucoma. II. The site of injury and susceptibility to damage. Arch Ophthalmol 99:635–649.
3. Burgoyne CF, JC Downs, AJ Bellezza, JK Suh and RT Hart. (2005). The optic nerve head as a biomechanical structure: a new paradigm for understanding the role of IOP-related stress and strain in the pathophysiology of glaucomatous optic nerve head damage. Prog Retin Eye Res 24:39–73.
4. Alvarado J, C Murphy and R Juster. (1984). Trabecular meshwork cellularity in primary open-angle glaucoma and nonglaucomatous normals. Ophthalmology 91:564–579.
5. Hamard P, F Valtot, P Sourdille, F Bourles-Dagonet and C Baudouin. (2002). Confocal microscopic examination of trabecular meshwork removed during ab externo trabeculectomy. Br J Ophthalmol 86:1046–1052.
6. Rasmussen CA and PL Kaufman. (2014). The trabecular meshwork in normal eyes and in exfoliation glaucoma. J Glaucoma 23:S15–S19.
7. Salowe RJ and JM O'Brien. (2014). NEI's audacious goals initiative. Ophthalmology 121:615–616.
8. Bang OY. (2016). Clinical trials of adult stem cell therapy in patients with ischemic stroke. J Clin Neurol 12:14–20.
9. Prockop DJ and SD Olson. (2007). Clinical trials with adult stem/progenitor cells for tissue repair: let's not overlook some essential precautions. Blood 109:3147–3151.

10. Du Y, DS Roh, MM Mann, ML Funderburgh, JL Funderburgh and JS Schuman. (2012). Multipotent stem cells from trabecular meshwork become phagocytic TM cells. Invest Ophthalmol Vis Sci 53:1566–1575.
11. Yun H, Y Zhou, A Wills and Y Du. (2016). Stem cells in the trabecular meshwork for regulating intraocular pressure. J Ocul Pharmacol Ther 32:253–260.
12. Du Y, H Yun, E Yang and JS Schuman. (2013). Stem cells from trabecular meshwork home to TM tissue in vivo. Invest Ophthalmol Vis Sci 54:1450–1459.
13. Yun H, Y Wang, Y Zhou, K Wang, M Sun, DB Stolz, X Xia, CR Ethier and Y Du. (2018). Human stem cells home to and repair laser-damaged trabecular meshwork in a mouse model. Commun Biol 1:216.
14. Yu WY, C Sheridan, I Grierson, S Mason, V Kearns, AC Lo and D Wong. (2011). Progenitors for the corneal endothelium and trabecular meshwork: a potential source for personalized stem cell therapy in corneal endothelial diseases and glaucoma. J Biomed Biotechnol 2011:412743.
15. Kim H, HY Kim, MR Choi, S Hwang, KH Nam, HC Kim, JS Han, KS Kim, HS Yoon and SH Kim. (2010). Dose-dependent efficacy of ALS-human mesenchymal stem cells transplantation into cisterna magna in SOD1-G93A ALS mice. Neurosci Lett 468:190–194.
16. Mendicino M, AM Bailey, K Wonnacott, RK Puri and SR Bauer. (2014). MSC-based product characterization for clinical trials: an FDA perspective. Cell Stem Cell 14:141–145.
17. Galipeau J. (2013). The mesenchymal stromal cells dilemma—does a negative phase III trial of random donor mesenchymal stromal cells in steroid-resistant graft-versus-host disease represent a death knell or a bump in the road? Cytotherapy 15:2–8.
18. Francois M, IB Copland, S Yuan, R Romieu-Mourez, EK Waller and J Galipeau. (2012). Cryopreserved mesenchymal stromal cells display impaired immunosuppressive properties as a result of heat-shock response and impaired interferon-gamma licensing. Cytotherapy 14:147–152.
19. Du Y, ML Funderburgh, MM Mann, N SundarRaj and JL Funderburgh. (2005). Multipotent stem cells in human corneal stroma. Stem Cells 23:1266–1275.
20. Kumar A, V Kumar, V Rattan, V Jha and S Bhattacharyya. (2017). Secretome cues modulate the neurogenic potential of bone marrow and dental stem cells. Mol Neurobiol 54: 4672–4682.
21. Kumar A, V Kumar, V Rattan, V Jha, A Pal and S Bhattacharyya. (2017). Molecular spectrum of secretome regulates the relative hepatogenic potential of mesenchymal stem cells from bone marrow and dental tissue. Sci Rep 7:15015.
22. Keller KE, SK Bhattacharya, T Borras, TM Brunner, S Chansangpetch, AF Clark, WM Dismuke, Y Du, MH Elliott, et al. (2018). Consensus recommendations for trabecular meshwork cell isolation, characterization and culture. Exp Eye Res 171:164–173.
23. Abbott A. (2014). Leaked files slam stem-cell therapy. Nature 505:139–140.
24. Kuriyan AE, TA Albini, JH Townsend, M Rodriguez, HK Pandya, RE Leonard, 2nd, MB Parrott, PJ Rosenfeld, HW Flynn, Jr. and JL Goldberg. (2017). Vision loss after intravitreal injection of autologous ''stem cells'' for AMD. N Engl J Med 376:1047–1053.
25. Trounson A and C McDonald. (2015). Stem cell therapies in clinical trials: progress and challenges. Cell Stem Cell 17:11–22.
26. Chambers DC, D Enever, N Ilic, L Sparks, K Whitelaw, J Ayres, ST Yerkovich, D Khalil, KM Atkinson and PM Hopkins. (2014). A phase 1b study of placenta-derived mesenchymal stromal cells in patients with idiopathic pulmonary fibrosis. Respirology 19:1013–1018.
27. Gupta N, RG Henry, J Strober, SM Kang, DA Lim, M Bucci, E Caverzasi, L Gaetano, ML Mandelli, et al. (2012). Neural stem cell engraftment and myelination in the human brain. Sci Transl Med 4:155ra137.
28. Le Blanc K, F Frassoni, L Ball, F Locatelli, H Roelofs, I Lewis, E Lanino, B Sundberg, ME Bernardo, et al. (2008). Mesenchymal stem cells for treatment of steroid-resistant, severe, acute graft-versus-host disease: a phase II study. Lancet 371:1579–1586.
29. Sachdeva N. (2009). Analysis of the viability of umbilical cord blood stem cells. J Stem Cells Regen Med 5:44–48.
30. Morgenstern DA, G Ahsan, M Brocklesby, S Ings, C Balsa, P Veys, P Brock, J Anderson, P Amrolia, et al. (2016). Post-thaw viability of cryopreserved peripheral blood stem cells (PBSC) does not guarantee functional activity: important implications for quality assurance of stem cell transplant programmes. Br J Haematol 174:942–951.
31. Kumar A, S Bhattacharyya and V Rattan. (2015). Effect of uncontrolled freezing on biological characteristics of human dental pulp stem cells. Cell Tissue Bank 16: 513–522.
32. Kumar A, Y Xu, E Yang and Y Du. (2018). Stemness and regenerative potential of corneal stromal stem cells and their secretome after long-term storage: implications for ocular regeneration. Invest Ophthalmol Vis Sci 59: 3728–3738.
33. Louis SA, RL Rietze, L Deleyrolle, RE Wagey, TE Thomas, AC Eaves and BA Reynolds. (2008). Enumeration of neural stem and progenitor cells in the neural colony-forming cell assay. Stem Cells 26:988–996.
34. Pastrana E, V Silva-Vargas and F Doetsch. (2011). Eyes wide open: a critical review of sphere-formation as an assay for stem cells. Cell Stem Cell 8:486–498.
35. Tay CY, P Sathiyanathan, SW Chu, LW Stanton and TT Wong. (2012). Identification and characterization of mesenchymal stem cells derived from the trabecular meshwork of the human eye. Stem Cells Dev 21:1381–1390.
36. Nadri S, S Yazdani, E Arefian, Z Gohari, MB Eslaminejad, B Kazemi and M Soleimani. (2013). Mesenchymal stem cells from trabecular meshwork become photoreceptor-like cells on amniotic membrane. Neurosci Lett 541:43–48.
37. Kelley MJ, AY Rose, KE Keller, H Hessle, JR Samples and TS Acott. (2009). Stem cells in the trabecular meshwork: present and future promises. Exp Eye Res 88:747–751.
38. McGowan SL, HF Edelhauser, RR Pfister and DR Whikehart. (2007). Stem cell markers in the human posterior limbus and corneal endothelium of unwounded and wounded corneas. Mol Vis 13:1984–2000.
39. Braunger BM, B Ademoglu, SE Koschade, R Fuchshofer, BT Gabelt, JA Kiland, EA Hennes-Beann, KG Brunner, PL Kaufman and ER Tamm. (2014). Identification of adult stem cells in Schwalbe's line region of the primate eye. Invest Ophthalmol Vis Sci 55:7499–7507.
40. Zhang Y, S Cai, SCG Tseng and YT Zhu. (2018). Isolation and expansion of multipotent progenitors from human trabecular meshwork. Sci Rep 8:2814.
41. Castro A and Y Du. (2019). Trabecular meshwork regeneration—a potential treatment for glaucoma. Curr Ophthalmol Rep 7:80–88.

42. Fisher JN, GM Peretti and C Scotti. (2016). Stem cells for bone regeneration: from cell-based therapies to decellularised engineered extracellular matrices. Stem Cells Int 2016: 9352598.
43. Morgan JT, JA Wood, NJ Walker, VK Raghunathan, DL Borjesson, CJ Murphy and P Russell. (2014). Human trabecular meshwork cells exhibit several characteristics of, but are distinct from, adipose-derived mesenchymal stem cells. J Ocul Pharmacol Ther 30:254–266.
44. Lunn JS, SA Sakowski, J Hur and EL Feldman. (2011). Stem cell technology for neurodegenerative diseases. Ann Neurol 70:353–361.
45. Yan J, L Xu, AM Welsh, G Hatfield, T Hazel, K Johe and VE Koliatsos. (2007). Extensive neuronal differentiation of human neural stem cell grafts in adult rat spinal cord. PLoS Med 4:e39.
46. Corti S, M Nizzardo, M Nardini, C Donadoni, S Salani, D Ronchi, F Saladino, A Bordoni, F Fortunato, et al. (2008). Neural stem cell transplantation can ameliorate the phenotype of a mouse model of spinal muscular atrophy. J Clin Invest 118:3316–3330.
47. Freeman TB, F Cicchetti, AC Bachoud-Levi and SB Dunnett. (2018). Technical factors that influence neural transplant safety in Huntington's disease. Exp Neurol 227: 1–9.
48. Wang H, M Wu, C Zhan, E Ma, M Yang, X Yang and Y Li. (2012). Neurofilament proteins in axonal regeneration and neurodegenerative diseases. Neural Regen Res 7:620–626.
49. Uchida A, T Tashiro, Y Komiya, H Yorifuji, T Kishimoto and S Hisanaga. (2004). Morphological and biochemical changes of neurofilaments in aged rat sciatic nerve axons. J Neurochem 88:735–745.
50. Foudah D, M Monfrini, E Donzelli, S Niada, AT Brini, M Orciani, G Tredici and M Miloso. (2014). Expression of neural markers by undifferentiated mesenchymal-like stem cells from different sources. J Immunol Res 2014: 987678.
51. Sathiyanathan P, CY Tay and LW Stanton. (2017). Transcriptome analysis for the identification of cellular markers related to trabecular meshwork differentiation. BMC Genomics 18:383.
52. Stamer WD, RE Seftor, RW Snyder and JW Regan. (1995). Cultured human trabecular meshwork cells express aquaporin-1 water channels. Curr Eye Res 14:1095–1100.
53. Stamer WD, K Peppel, ME O'Donnell, BC Roberts, F Wu and DL Epstein. (2001). Expression of aquaporin-1 in human trabecular meshwork cells: role in resting cell volume. Invest Ophthalmol Vis Sci 42:1803–1811.
54. Wang Y, D Osakue, E Yang, Y Zhou, H Gong, X Xia and Y Du. (2019). Endoplasmic reticulum stress response of trabecular meshwork stem cells and trabecular meshwork cells and protective effects of activated PERK pathway. Invest Ophthalmol Vis Sci 60:265–273.
55. Raghunathan VK, JT Morgan, SA Park, D Weber, BS Phinney, CJ Murphy and P Russell. (2015). Dexamethasone stiffens trabecular meshwork, trabecular meshwork cells, and matrix. Invest Ophthalmol Vis Sci 56:4447–4459.
56. Russell P and M Johnson. (2012). Elastic modulus determination of normal and glaucomatous human trabecular meshwork. Invest Ophthalmol Vis Sci 53:117.
57. Kuchtey J, ME Kallberg, KN Gelatt, T Rinkoski, AM Komaromy and RW Kuchtey. (2008). Angiopoietin-like 7 secretion is induced by glaucoma stimuli and its concentration is elevated in glaucomatous aqueous humor. Invest Ophthalmol Vis Sci 49:3438–3448.
58. Comes N, LK Buie and T Borras. (2011). Evidence for a role of angiopoietin-like 7 (ANGPTL7) in extracellular matrix formation of the human trabecular meshwork: implications for glaucoma. Genes Cells 16:243–259.

Address correspondence to:
Dr. Yiqin Du
Department of Ophthalmology
University of Pittsburgh
203 Lothrop Street
Pittsburgh, PA 15213

E-mail: duy@upmc.edu

Received for publication August 7, 2019
Accepted after revision November 1, 2019
Prepublished on Liebert Instant Online November 2, 2019